Numerical and experimental analysis of mechanical and fatigue properties of special shaped 3D printed sample

David Juračka, David Bujdoš, Petr Lehner
VSB – Technical University of Ostrava, Faculty of Civil Engineering, Czech Republic
david.juracka@vsb.cz, https://orcid.org/0000-0001-8252-6433
david.bujdos@vsb.cz
petr.lehner@vsb.cz, http://orcid.org/0000-0002-1478-5027

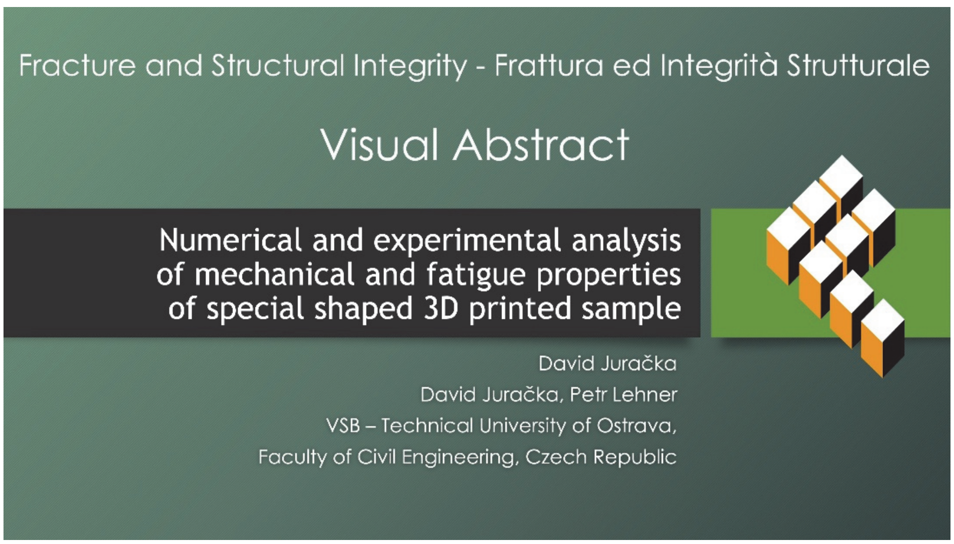

OPEN ACCESS

Citation: Juracka, D., Bujdos, D., Lehner, P., Mechanical and fatigue analysis of special shape of 3D printed sample, Fracture and Structural Integrity, 74 (2025) 415-421.

Received: 30.07.2025
Accepted: 03.09.2025
Published: 21.09.2025
Issue: 10.2025

KEYWORDS. Numerical modeling, Shear, Fatigue, 3D print, Experiment.

INTRODUCTION

In recent years and decades, the construction industry has faced new problems and challenges that require innovative technologies and approaches to solve them. One such approach is 3D printing. Materials such as concrete, metal or polymers can be used to create 3D structures [4,12]. Unlike the use of concrete, the use of 3D printing of metal or polymer materials for structural support elements is less widespread and represents an area that has not been explored much. 3D printing is an additive process that adds material to the desired final shape. The most commonly used technology for 3D printing plastics is Fused Deposition Modeling (FDM), which works very simply [13]. An object is created layer by layer by melting a thin strip of plastic (or metal) material. The advantages of FDM include simplicity, minimal waste, ease of designing models of various sizes, usability of a wide range of materials, and applicability to even very inexpensive printers. On the other hand, disadvantages include lower quality print detail, large layer thicknesses, imperfections, and ambiguity in the durability of the product itself [18]. Given these disadvantages, construction professionals must question whether this technology is appropriate. The answer, of course, is not simple, but there is certainly room to evaluate the appropriate use of FDM technology in construction and the like. As mentioned, 3D concrete printing has already secured its place [5] and is being used despite many challenges around the world. In contrast, 3D printing of other materials in the construction industry is limited. We can find only a few real examples that show a strong commitment to interesting design and modern concepts in the industry [6–8,14]. The cornerstone of research on 3D printing in construction can be numerical modelling using the finite element method (FEM) [2]. It is less time demanding and more economical solution. On the other hand, the calibration of such models is complex and heavily dependent on the correct description of material properties. The beginnings of the research program were presented, for example, in earlier articles [3,8]. The present paper demonstrates the inverse analysis process on two sets of specimens with different geometries that have been experimentally evaluated. By successively adjusting the material parameters, a high agreement of the force-displacement diagram results was achieved. After demonstrating the agreement between the numerical model and the experimental results, a simplified fatigue analysis was performed. The aim of the article is to determine the service life and durability of a specially shaped specimen, which was developed for the purpose of effective material optimization, by combining numerical modeling and experimental testing.

THEORETICAL AND EXPERIMENTAL BACKGROUND

3D printing in structural engineering

Despite its undeniable advantages, including speed and a large shape range, 3D printing has several disadvantages that need to be taken into account. These include fragility and susceptibility to fracture problems, as well as instability of material properties [11,17]. Nowadays, several methods are used, differing in the material and technology used. For example, it can be FDM (fused deposition modelling), SLA (stereolithography) or SLS (selective laser sintering) [19]. Each of these methods has its advantages and disadvantages in terms of accuracy, speed, cost and final product properties. Furthermore, the extension of applicability to different applications and problems can be seen [20].

Mechanical and fatigue behaviour of 3D printed samples

3D printed samples exhibit different mechanical and fatigue parameters compared to conventionally processed materials. Fatigue life is influenced by the microstructure of the print layers, orientation, and any defects [1]. The number of cycles before final failure is significantly influenced by the print speed and sensitivity settings [9]. A significant shift towards higher mechanical and fatigue resistance can be achieved by changing the print geometry, i.e., optimizing the layering and orientation of the layers [1]. The presented study builds on these findings and provides further insight using numerical models.

Previous research

The research is based on several published studies that have analysed the mechanical properties of 3D printed materials using FFF/FDM technologies [3,8,10]. FFF/FDM 3D printed components made of plastic materials are generally not suitable as primary load-bearing joints in wood or steel structures unless carefully designed for load-bearing and long-term durability. However, they can serve as auxiliary elements, e.g. for spacers, informal joints or temporary structures where high load-bearing capacity and durability are not the main requirements. In cases where a strength solution is required, higher quality materials or other manufacturing technologies can be used. At the same time, a hybrid approach can be considered, such as combining 3D printing with different materials (filler and high-strength material) or with metal reinforcements and other materials.

EXPERIMENTS AND NUMERICAL MODELS

Geometry and printing

The tests were carried out on an electromechanical machine where the samples were clamped in jaws and the press introduced deformation. A record of the force and deformation was provided for further evaluation. Two groups of results were evaluated separately - the strain on a conventional specimen (see Fig. 1 (a)) and the strain on a specially designed specimen geometry (see Fig. 1 (b)). The standard sample is 180 mm long, 20 mm wide and 4 mm thick. The second

specimen had a more complex geometry that was created to create areas of shear. It is 170 mm long, 20 mm wide and 11.6 mm thick. A printing with a size of layers 0.2 by 0.4 mm was chosen for these samples.
The basic dimensions (in mm) of the special shape of the specimen are presented in the drawing in Fig. 2a. Fig. 2b shows a detail of the model in the Prusa printing program [15]. For the first set of data, the normal shape tensile test, 5 experimental results and numerical models created in Ansys 2024 R2 [15] were used. The geometry was prepared at a scale of 1:1. The second set included only one experiment, as the production of a special specimen was time and cost consuming.
The experimental test used an electromechanical machine FP-10 with a setting of the speed of the gripping jaws moving away from each other of 1 mm per minute.

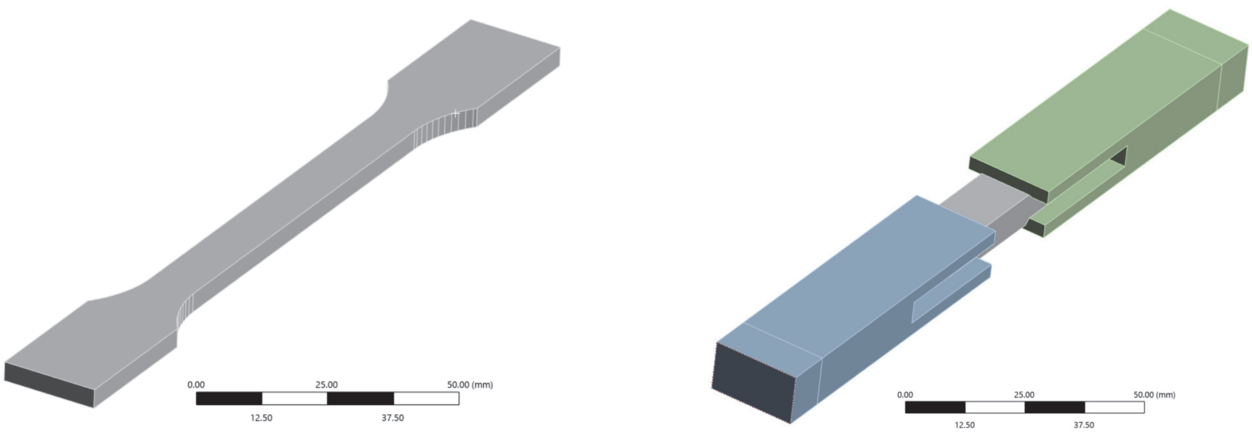

(a) Model A (b) Model B

Figure 1: Printed 3D element (a) standard geometry of model A for tensile test, (b) special geometry of model B for shear tensile test.

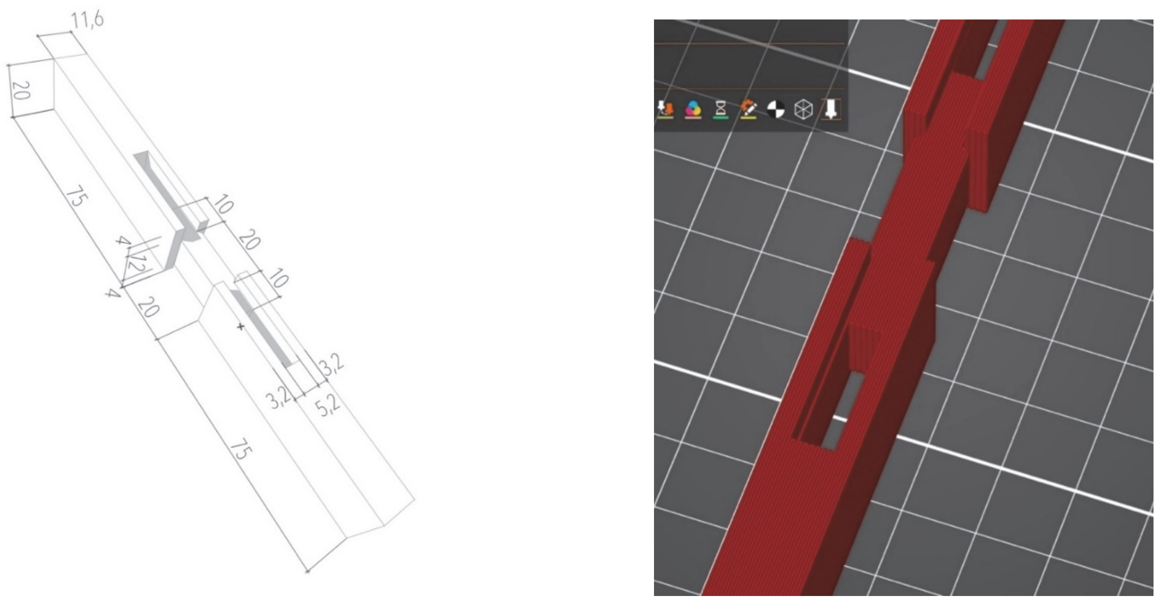

(a) (b)

Figure 2: Special printed 3D element of model B (a) dimensions, (b) detail of layers.

Numerical and material model

In order to obtain accurate material parameters of 3D printed elements, an inverse analysis was prepared based on the comparison of experimental results and numerical finite element (FEM) models. The boundary conditions corresponded to the exact test setup. The model contains approximately 13 000 nodes and 11 000 elements. The material constants: elastic modulus, Poisson's constant and yield strength were parametrically adjusted in the study. In the material model A, the following material properties are set for the 3D printed element: modulus of elasticity in tension is 1.9 GPa, tensile strength is 63 MPa, Poisson's constant is 0.4 and density is 1220 kg/m^3. These parameters were obtained from the technical data sheet of the filament manufacturer. In model B, new parameters were obtained by inverse analysis based on the comparison of force-displacement diagram from the experiment. The aim was to approximate the behaviour of the samples as closely as possible. These material parameters were included in the system as variables and thus cyclic input of properties and comparison of results could be used. Model B is therefore the result of this parametric inverse analysis.

Fatigue analysis

The aim of the next analysis was to evaluate the critical fatigue points on the 3D printed sample. The loading force was determined from the first loading scheme. Cyclic loading is then used to estimate the service life. Loading was performed using an amplitude of the magnitude of the force at the level of the maximum stress at the critical point. The critical stresses on the elements were compared with the S-N curve for polycarbonate (see Fig. 3) [16]. From the obtained value of the number of cycles, it is possible to determine the critical points, and which geometry variant has better resistance.

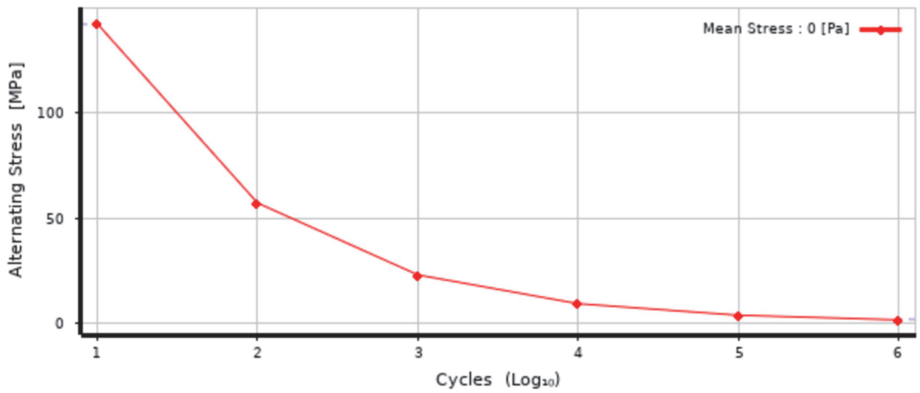

Figure 3: S-N curve for polycarbonate.

Results

Inverse analysis of material properties

As mentioned above, the outputs from the numerical models were compared with the experimental results. Two sets of results are analysed: a standard-shaped tensile test body and a shear-dominated tensile test body. Fig. 4 presents the force-displacement diagrams for the standard sample. As mentioned above, the outputs from the numerical models were compared with the experimental results. Two sets of results are analysed: a standard-shaped tensile test body and a shear-dominated tensile test body. There are five plots from experimental tests and two numerical models. Model A has the basic parameters; model B has the parameters obtained by inverse analysis. The graphs show a great similarity in behaviour.

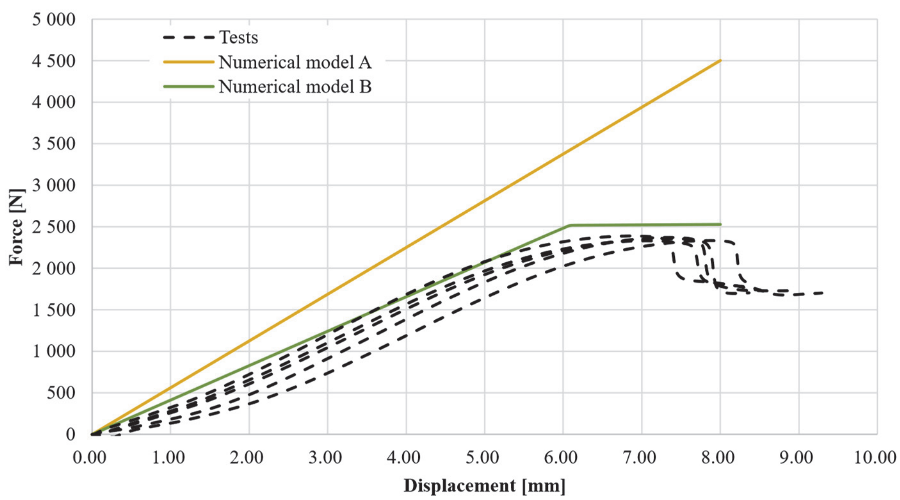

Figure 4: Force-displacement diagrams from physical tests and numerical models of standard sample.

The second plot in Fig. 5 shows a comparison of the force-displacement diagram for the special shape sample from the second set. Only one test was performed, but the numerical modelling process was the same as for the first set. The difference at the beginning is most likely due to the slippage of the specimens, which led to a larger increase in strain at a smaller force. The slope of the curves is very similar for the test and model B, and the maximum value at which failure occurred in the real world and the rapid increase in plastic deformation occurred in the model is similar.

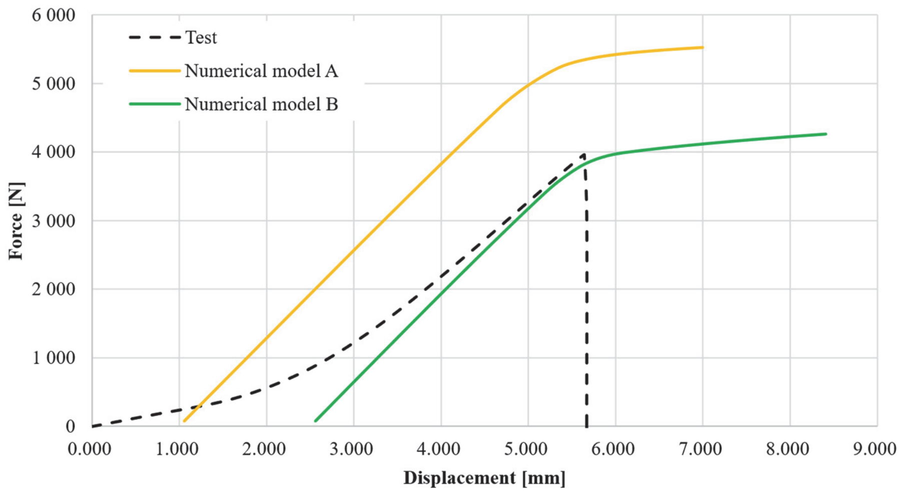

Figure 5: Force-displacement diagrams from physical tests and numerical models of special sample.

Comparison of sample failure

A comparison of the failure of a special 3D printed element was also performed. Fig. 5 (a) shows a post-test photograph showing the separation at the junction of the inner and outer structures. Similarly, the graphical output of the equivalent plastic strain numerical model shows the locations where the specimen was expected to fail and separate during the tensile test.

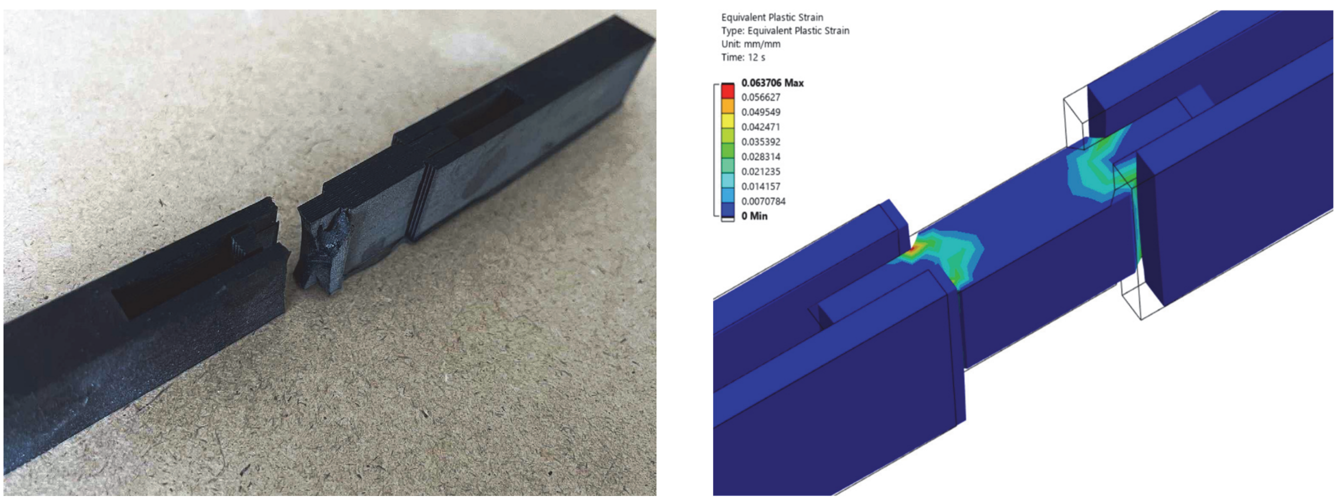

(a) (b)

Figure 6: Special printed 3D element (a) after experiment, (b) detail of equivalent plastic strain from numerical model.

Simplified fatigue analysis

Further results are represented by the number of load cycles in each element (node) of the 3D printed joint (see Fig. 7). This is a greatly simplified analysis, but it is very useful to understand the behavior of the sample itself depending on the shape. It can be seen that the stress concentrators are at the edge level of the inner and outer structures. With a load cycle set to the stress level at which the sample plasticizes, the minimum lifetime is 41 cycles. The color scale is divided decimally, so that it is possible to observe critical points that are like the real rupture point. It should be noted that the sample was manufactured continuously, and the sample does not contain any glued parts or joints.

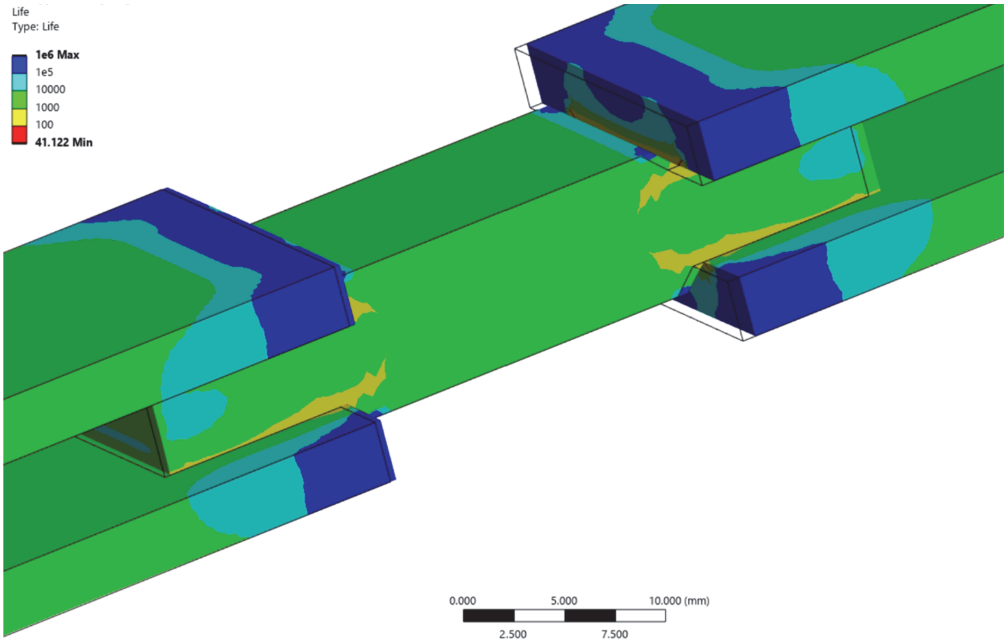

Figure 7: Visualization of fatigue life prediction.

Conclusions

This study presents a combined analysis of the mechanical and fatigue properties of specially shaped 3D printed specimens, with an emphasis on the calibration of numerical models with experimental results. Using inverse analysis, the material parameters in the numerical model were optimized to more accurately simulate the behavior of the specimens under tensile loading, both for standard and specially designed geometries. The results show good agreement between the experimental data and the numerical models, confirming the effectiveness of the methodology used. Subsequent simplified fatigue analysis, based on S-N curves for polycarbonate, revealed critical stress concentration points and predicted the service life of the specimens. The results obtained indicate that the geometry of the specimen significantly affects the fatigue resistance, with specially designed geometry showing potential for specific applications. This work highlights the importance of combining experimental and numerical methods for understanding the behavior of 3D printed materials and provides valuable insights for their use in structural applications, especially in the area of design optimization for improving mechanical and fatigue properties.

Acknowledgment

This research and this paper were funded by the Ministry of Education, Youth and Sports of the Czech Republic in Student Grant Competition through VSB – Technical University of Ostrava – grant number: SGS SP2025/075.

References

[1] Bakhtiari, H., Aamir, M., Tolouei-Rad, M. (2023). Effect of 3D Printing Parameters on the Fatigue Properties of Parts Manufactured by Fused Filament Fabrication: A Review, Applied Sciences (Switzerland). DOI: https://doi.org/10.3390/app13020904.

[2] Bathe, K.-J. (2008). Finite Element Method., Wiley Encyclopedia of Computer Science and Engineering, Hoboken, NJ, USA, John Wiley & Sons, Inc.
[3] Dedek, J., Juračka, D., Bujdoš, D., Lehner, P. (2024). Mechanical Properties of Wooden Elements with 3D Printed Reinforcement from Polymers and Carbon, Materials, 17(6). DOI: https://doi.org/10.3390/ma17061244.
[4] Dizon, J.R.C., Espera, A.H., Chen, Q., Advincula, R.C. (2018). Mechanical characterization of 3D-printed polymers, Addit Manuf. DOI: https://doi.org/10.1016/j.addma.2017.12.002.
[5] Federowicz, K., Techman, M., Skibicki, S., Chougan, M., El-Khayatt, A.M., Saudi, H.A., Błyszko, J., Abd Elrahman, M., Chung, S.Y., Sikora, P. (2023). Development of 3D printed heavyweight concrete (3DPHWC) containing magnetite aggregate, Mater Des, 233. DOI: https://doi.org/10.1016/j.matdes.2023.112246.
[6] Garzon-Hernandez, S., Garcia-Gonzalez, D., Jérusalem, A., Arias, A. (2020). Design of FDM 3D printed polymers: An experimental-modelling methodology for the prediction of mechanical properties, Mater Des, 188. DOI: https://doi.org/10.1016/j.matdes.2019.108414.
[7] Ghanbari-Ghazijahani, T., Kasebahadi, M., Hassanli, R., Classen, M. (2022). 3D printed honeycomb cellular beams made of composite materials (plastic and timber), Constr Build Mater, 315. DOI: https://doi.org/10.1016/j.conbuildmat.2021.125541.
[8] Juracka, D., Kawulok, M., Bujdos, D., Krejsa, M. (2022). Influence of Size and Orientation of 3D Printed Fiber on Mechanical Properties under Bending Stress, Periodica Polytechnica Civil Engineering, 66(4). DOI: https://doi.org/ 10.3311/PPci.19806.
[9] Khan, M.K.A., Alshahrani, H., Arun Prakash, V. (2023). Effect of grid pattern and infill ratio on mechanical, wear, fatigue and hydrophobic behaviour of abaca bracts biocarbon-ABS biocomposites tailored using 3D printing, Biomass Convers Biorefin. DOI: https://doi.org/10.1007/s13399-023-05196-4.
[10] Lehner, P., Pařenica, P., Juračka, D., Krejsa, M. (2024). Numerical analysis of 3D printed joint of wooden structures regarding mechanical and fatigue behaviour, Fracture and Structural Integrity, 19(71), pp. 151–163. DOI: https://doi.org/10.3221/IGF-ESIS.71.11.
[11] Majid, F., Hachimi, T., Rhanim, H., Rhanim, R. (2022). Delamination effect on the mechanical behavior of 3D printed polymers, Frattura Ed Integrità Strutturale, 17(63), pp. 26–36. DOI: https://doi.org/10.3221/IGF-ESIS.63.03.
[12] Marsavina, L., Dohan, V., Galatanu, S.-V. (2024). Mechanical Evaluation of Recycled PETG Filament for 3D Printing, Frattura Ed Integrità Strutturale, 18(70), pp. 310–321. DOI: https://doi.org/10.3221/IGF-ESIS.70.18.
[13] Maszybrocka, J., Dworak, M., Nowakowska, G., Osak, P., Łosiewicz, B. (2022). The Influence of the Gradient Infill of PLA Samples Produced with the FDM Technique on Their Mechanical Properties, Materials, 15(4). DOI: https://doi.org/10.3390/ma15041304.
[14] Nicolau, A., Pop, M.A., Coşereanu, C. (2022). 3D Printing Application in Wood Furniture Components Assembling, Materials, 15(8). DOI: https://doi.org/10.3390/ma15082907.
[15] Prusa i3. (2022). Original Prusa i3 MK3S+ 3D printer | Original Prusa 3D printers directly from Josef Prusa. PRUSA Research.
[16] Puigoriol-Forcada, J.M., Alsina, A., Salazar-Martín, A.G., Gomez-Gras, G., Pérez, M.A. (2018). Flexural fatigue properties of polycarbonate fused-deposition modelling specimens, Mater Des, 155. DOI: https://doi.org/DOI: 10.1016/j.matdes.2018.06.018.
[17] Sánchez, M., Arrieta, S., Cicero, S. (2023). Fracture Load Estimations for U-Notched and V-Notched 3D Printed PLA and Graphene-Reinforced PLA plates using the ASED Criterion, Frattura Ed Integrità Strutturale, 17(66), pp. 322–338. DOI: https://doi.org/10.3221/IGF-ESIS.66.20.
[18] Skoratko, A., Katzer, J. (2021). Harnessing 3d printing of plastics in construction—opportunities and limitations, Materials. DOI: https://doi.org/10.3390/ma14164547.
[19] Su, A., Al'Aref, S.J. (2018). History of 3D Printing, 3D Printing Applications in Cardiovascular Medicine, pp. 1–10. DOI: https://doi.org/10.1016/B978-0-12-803917-5.00001-8.
[20] Tomei, V., Grande, E., Imbimbo, M. (2024). Optimization of the internal structure of 3D-printed components for architectural restoration, Frattura Ed Integrità Strutturale, 18(70), pp. 227–241. DOI: https://doi.org/10.3221/IGF-ESIS.70.13.